LA-UR-19-32550
Approved for public release; distribution is unlimited.

Title: Comprehensive Data Analysis and Analytic Method Development for PBX9501 Material (FY2019 Annual Report of Aging and Lifetimes Program)

Author(s): Yang, Dali
Edgar, Alexander Steven
Adams, Jillian Cathleen
Torres, Joseph Angelo

Intended for: Report

Issued: 2020-03-24 (rev.1)

Comprehensive Data Analysis and Analytic Method Development for PBX9501 Material (FY2019 Annual Report of Aging and Lifetimes Program) (LA-UR-19-32550)

Dali Yang, Alex Edgar, Jillian Adams, and Joseph Torres
MST-7: Engineered Materials
Material Sciences and Technology Division
Los Alamos National Laboratory, Los Alamos, NM 87545
(dyang@lanl.gov, 505-665-4054)

Executive Summary

In the polymer bonded explosive (PBX) 9501, a binder consisting of 2.5 wt% nitroplasticizer (NP) and 2.5 wt% Estane®5703 (Estane) is combined with 94.9 wt% of the high-explosive HMX and 0.1 wt% stabilizer. Because of its flexibility and tensile strength, this binder lowers the sensitivity and improves the manufacturability of PBX 9501. However, like many plasticizers comprised of low molecular weight components, NP has a tendency to diffuse out of the PBX 9501 matrix and can decompose at moderate temperatures into reactive byproducts, such as NO, NO_2, H_2O, and HNO_x. Through oxidation and hydrolysis, these molecules can further degrade NP and Estane, ultimately degrading the properties of PBX 9501. While gaseous molecules can readily diffuse out of the PBX 9501 charges, the intermediates with lower volatility are more likely trapped in the condensed phase inside the charges and, in a closed system, will co-exist with Estane for an extended period of time creating an ongoing reactive environment. Understanding the rates of formation for these volatiles and intermediates during the NP degradation is therefore a critical prerequisite for understanding the long-term stability of polymeric binders used in munition systems. To work toward this ultimate goal, in the past year, we have conducted comprehensive studies on the physical properties of NP and finished three-year long aging experiment to understand the aging behavior of NP under thermal treatment. Important results are summarized in this annual report.

Although NP is widely used in the DOE complex, their physical properties are rather scattered and inconsistent in the open literature. For example, there are at least two widely different values, 14.5°C and -15°C, for the melting point of NP. Although it is known that NP is a eutectic 50:50 mixture of BDNPA and BDNPF, their eutectic phase diagram is not well documented. Furthermore, the effect of temperature on the miscibility between water and eutectic BDNPA/F mixture is rarely reported. To fill these knowledge gaps, a large set of BDNPA/F mixtures with BDNPA concentration ranging from 0 to 100 wt% was analyzed using DSC techniques. In addition to determining the eutectic melt point as -25°C, a phase diagram of the BDNPA/F system was constructed from -30°C to 45°C. With this phase diagram, the phase transition temperatures and composition can be readily found for the BDNPA/F mixtures with various mass ratios. The results are summarized in Part One.

During PBX 9501 production and its late characterization, the material is often directly in contact with water. While extensive characterization has been conducted on aged PBX 9501 as a whole, how NP degrades in direct contact with water has been rarely reported, therefore NP was aged in direct contact with water molecules in this study. To study the miscibility between NP and water, a large set of NP/water samples with water concentration ranging from 500 to 5800 ppm was fully characterized using coulometric Karl Fischer (KF) titration, TGA, DSC, and Near-IR Spectroscopy. From these data, a phase diagram of the NP and rich NP-water system was constructed from −90 to 130°C. From this phase

diagram, one can find the miscibility between NP and water changes significantly with temperature and mixing conditions. Heating increases the homogeneity threshold and water solubility in NP. For example at 22°C, NP can potentially contain as high as 3560 ppm when NP directly contacts water. Since water molecules can hydrolytically degrade Estane, which ultimately degrades the chemical and mechanical properties of the polymer, the phase diagram of NP and water mixtures can be an important tool in estimating potential water concentration in NP and the other materials with the presence of NP at different temperatures. These results are summarized in Part One as well.

Although numerous aging studies of PBX9501 have been conducted, there are many questions which remain unanswered. For example, why does the same PBX9501 used in the different systems give different degradation behaviors? To address this question, the NP thermal stability has been blamed to cause the degradation of Estane in PBX 9501 for some systems. It is known that NP stored at Pantex for more than 50 years still met the specification for the PBX9501 production. It seems to be commonly believed that NP is a stable chemical when it is stored at ambient conditions. Clearly, NP becomes unstable when it is exposed to elevated temperatures, which we had demonstrated in our recent studies. However, we still need to know how and at what conditions the NP degradation starts. Temperature and headspace composition are two major factors that impact the NP aging behavior. Although temperature control is relatively easy to achieve, mimicking the headspace conditions to simulate weapon applications is more difficult. In our previous studies conducted between 2010 – 2014, the effects of temperature and composition on the NP degradation have been systematically examined, and profound knowledge about the NP degradation has been accumulated. However, in this earlier work, the aging containers had a large free volume (>30x the NP volume). This was not representative of weapon conditions, where the systems are sealed with a very small free volume. To understand how NP degrades in weapon applications, we conducted a three year-long aging experiment and investigated the aging behavior in systems with low free volume in various atmospheres (dry and wet) at temperatures 70°C and below. The properties of aged samples were analyzed using TGA, KF titration, and FTIR spectroscopy over a period of three years. We found when NP ages inside a confined system, there seems to be a transition at around 55°C at which the aging behavior of the NP changes. Below 55°C, a trace amount of water (>550 ppm) stabilizes the properties of NP by preventing HONO formation. Above 55°C, nitrous acid (HONO) formation - the first step in NP degradation and decomposition - starts within a few months, regardless of the exposed compositions. On the nature of the degradation mechanism itself, it is suspected that the formed NO_x and water from the HONO decomposition serve to auto-catalyze the NP degradation, which results in irreversible NP degradation. Since the amount of water (and volatiles) involved in the initial degradation of NP is on the order of a few hundred ppms, it becomes critical to rigorously control headspace volume to study the aging behavior of NP and NP contained materials, such as PBX 9501. Over the past two decades, numerous artificial aging experiments of PBX 9501 and polymeric materials containing NP have been conducted in the DOE complex at temperatures up to 80°C, without and with humidity [up to 75 relative humidity (RH) %], often with a large headspace volume in the aging containers, and sometimes with an extra NP source. Although invaluable knowledge has been accumulated about the aging behaviors of these materials and the hydrolysis of Estane is now well understood, the uncovered aging behaviors are not necessarily relevant to our applications. We hope that the results obtained from this new study shed some light on the conditions at which NP degradation starts and provides experimental evidence which may help guide the design of future artificial aging studies related to the materials containing NP under conditions more relevant to weapon applications. These results are summarized in Part Two.

Over the years, the characterization of BDNPA/F is typically conducted using a conventional high-performance/pressure liquid chromatography (HPLC) technique. The focus on this characterization is the concentration of BDNPA/F as chemical constituents in the aged PBX 9501 materials. Their identifications are based on their retention (elution) times HPLC columns by assuming that their properties remain unchanged over the aging process. In this methodology the chemical functionality of BDNPA/F is not characterized. However, more and more core surveillance data suggest that the BDNPA/F have aged differently when the PBX9501 charges are aged in different LANL weapon systems. Clearly, the conventional HPLC method is not sufficient for BDNPA/F characterization if their properties change over the aging process. In FY2018, we purchased a high resolution HPLC/MS/MS system - SCIEX X500r liquid chromatography tandem quadrupole time of flight (LC-QTOF) instrument. By using different ionization modes, this sophisticated system can be an excellent tool to identify unknown fragments from the degradation of polymer (<40kDa) to small molecules (>20 Da). We believe that its implementation in the binder characterization of PBX9501 will provide rich scientific insights on the degradation pathways of NP and other molecules when the binder molecules are aged inside the PBX 9501 charges. In FY2019, we have been focusing on methodology development for BDNPA/F characterization. The degraded NP samples obtained from the above aging experiment are used for method development. Since the information obtained from this instrument is rather overwhelming, continued efforts in FY2020 will be dedicated to refine the developed methodology and to develop effective data processing method so that the wealth of data can be processed and presented effectively. The ultimate goal is to reveal the mechanisms of NP and Estane degradation when they are aged inside PBX 9501 charges used in the LANL weapon systems. Preliminary results obtained in FY2019 will be presented in Part Three of this report.

Part One: Comprehensive Characterization of Nitroplasticizer Physical Properties

Nitroplasticizers are commonly used to plasticize polymers so to enhance adhesion of polymer to highly energetic crystals, such as HMX (octahydro-1,3,5,7-tetranitro-1,3,5,7-tetrazocine), while maintaining energetic potential of the composite. Therefore, the mixture of nitroplasticizer and polymer can be used as an effective binder in polymer bonded explosives (PBX) 9501, which enhances the machinability of the PBX for numerous civil, oil field, and military applications [1-5]. One pair of commonly used nitroplasticizers is bis-2,2-dinitropropyl acetal (BDNPA) and bis-2,2-dinitropropyl formal (BDNPF). While the individual melt temperatures (T_m) of BDNPA or BDNPF are above 30°C, mixing a 1:1 mass ratio of BDNPA/F forms a eutectic mixture with the lowest possible T_m, which greatly extends its plasticization temperature and hence its plasticization effect on the polymer [1, 6, 7]. Although BDNPA and BDNPF can be used separately to mix with polymer as a binder in a PBX, their eutectic mixture with 1:1 mass ratio (hereinafter called BDNPA/F or NP) is used preferentially because of its plasticization effect and improved the functionality of the binder material. Despite their wide applications, the physical properties of BDPNA, BDNPF, and BDNPA/F in the literature are rather scattered and inconsistent. For example, inconsistency was found in the literature about the melt temperature of the eutectic point of BDNPA/F. In 1973, T. Rivera reported a phase diagram of the BDNPA/F system between 0 and 40°C [7]. The eutectic composition is ~51% of BDNPA with the melting point of ~14.5°C. Contrarily, several studies reported the melting point of eutectic BDNPA/F (1:1 mass ratio) as -15°C [4, 5]. The discrepancy in this eutectic melting temperature is rather large. Furthermore, the eutectic phase diagram of the BDNPA/F mixtures is not well documented [7]. To resolve these discrepancies, the T_ms of the eutectic BDNPA/F mixtures and the phase diagram of the BDNPA/F system were carefully determined. Since the detailed description of this work is given in one of our recent manuscripts [8], only the brief description of their physical properties is given below.

1.1 Heat fusion of BDNPA and BDNPF

From DSC measurements, the heat fusion (ΔH_f) of the Pantex BDNPA/F samples were determined, as listed in Table 1. Considering their purities, the values were adjusted to the 100% purity of BDNPA and BDNPF. In 1973, T. Rivera determined the ΔH_f of BDNPA and BDNPF [10]. These literature values are listed in Table as well. Clearly, there is a difference between these two sets of data. It is suspected that the inconsistency comes from the impurities of different BDNPA and BDNPF sources.

Table 1. Heat of fusion and physical properties of BDNPA and BDNPF.

Sample	Density of pure compound (g/cm^3)*	Molar mass of pure compound (g/mol)	Measured ΔH_f (kcal/mol)	Literature ΔH_f (kcal/mol)**	Difference (%)
BDNPA	1.366	326.22	6.16	6.70	8.46
BDNPF	1.411	312.19	5.54	6.04	7.97

*from [1], ** from [7]

1.2 The Phase diagram of BDNPA and BDNPF mixture

The phase diagram of BDNPA and BDNPF mixture, as shown in Figure 1, is comprised of four distinct phases: one contains only liquid, one only solids, and two of them contain liquids and solids. In the field of F + A + FA, the material is composed of three phases of solids: crystalline BDNPA, crystalline BDNPF, and crystals composed of various combinations of BDNPA and BDNPF. No strong evidence of a solvus for either material was detected. A fifth phase is known, however this amorphous solid phase is not shown in the diagram. The phase boundary, based on the detected glass transition, is a straight line from -68.7°C in the purest BDNPF to -65.5°C in the purest BDNPA. At temperatures below the glass transition, this solid phase is comprised of the ordered solids described above and a disordered amorphous solid of BDNPA and BDNPF. Although the boundary between this fifth and the F + A + FA phases is well defined in the data, it has been omitted from the phase diagram because it contributes little to the practical use of the material. Based on the modulated differential scanning calorimetry (MDSC) results of this study, the eutectic point of the BDNPA/F system is -25.9°C at 52.3% BDNPA and 47.7% BDNPF. Despite the apparent difference in these from the values reported by Shen 1991 and Wingborg 2002 [5, 9], the numbers agree. Previous authors were likely reporting the onset of crystallization on cooling (-15°C) and we are reporting the maxima of change in heat capacity at thermal transitions (-25.9°C). With this phase diagram, the phase transition temperatures and composition can be readily found for the BDNPA/F system with various mass ratios. The detailed description on how this phase diagram was constructed can be found in reference [8].

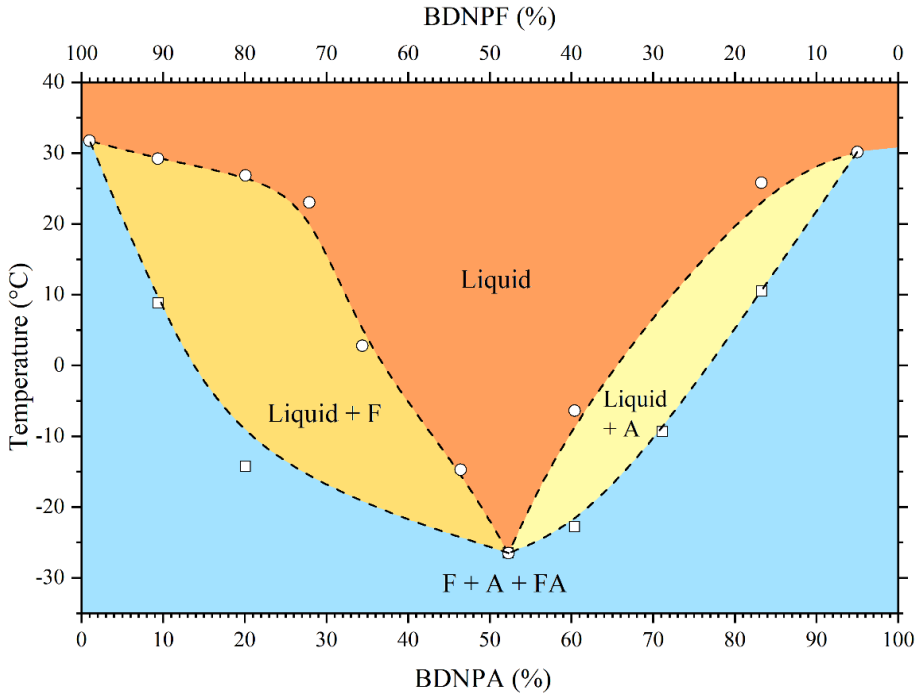

Figure 1. Eutectic phase diagram of BDNPA-BDNPF, F= solid BDNPF, A=solid BDNPA, and FA=solid BDNPA and BDNPF.

1.3 The Phase diagram of NP and NP rich-water mixture

In PBX9501, the polymer chain length directly correlates to the overall mechanical strength of the polymer, therefore polymer degradation rates are important for the safe use of the material [10]. Polymer hydrolysis is a well-known phenomenon [11] and upon hydrolyzation, polymers often lose their

mechanical integrity. Poly(ester urethane), such as Estane®5703 (Estane), is used as a binder in the formulation of PBX. Previous studies suggest hydrolyzation driven chain scission is one of the main degradation pathways. Excessive water causes acid formation in BDNPA/F. When Estane is in contact with BDNPA/F, the result is acid catalyzed hydrolysis of Estane and chain scission along the ester backbone [12, 13]. However, scarce water also degrades BDNPA/F, producing H_2O and NO_x [14], resulting in oxidative crosslinking and non-hydrolytic chain scission of Estane in addition to the hydrolytic chain scission [2, 13, 15-17, 21]. Both conditions result in undesirable changes in the chemical/thermal/mechanical properties of Estane and PBX 9501 materials. Due to the degradative effect of excess/scarce water on the polymeric binder and BDNPA/F, determination of the water content in NP, NP plasticized Estane, and PBX 9501 is crucial. As water sorption in both HMX and Estane have been studied previously [17], this study focuses on the miscibility of water in NP and water solubility in NP, specifically in constructing the NP rich NP-water phase diagram. Again, since the detailed description how to construct this phase diagram is given in one of our recent manuscripts [8], only the phase diagram of NP and water is presented below.

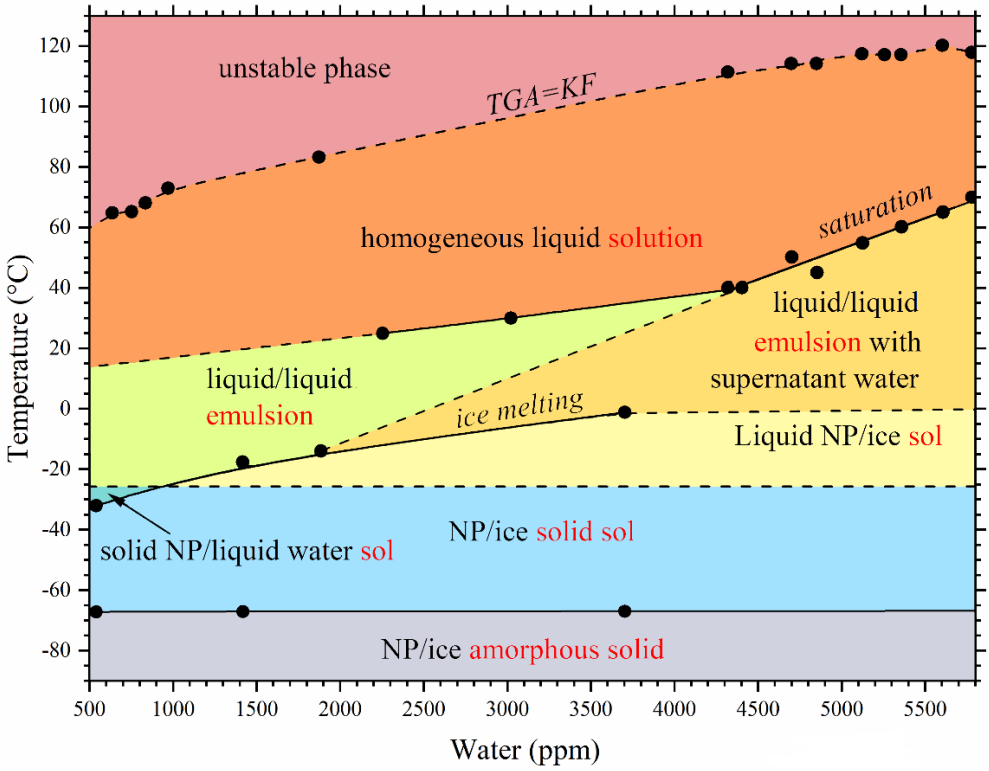

Figure 2. The temperature dependent phase diagram of NP rich, NP-water mixture. Dashed lines represent transitions dependent on experimental conditions or extrapolations.

From the phase diagram of NP and water mixtures, it was found the miscibility between NP and water changes significantly with temperature and mixing conditions. Furthermore, despite the water concentration in the NP, on heating from < -67°C, the phases will pass through a solid state, at least one sol phase, an emulsion phase, into a homogeneous phase, and finally into an unstable phase. Heating increases the homogeneity threshold and water solubility in NP. At 22°C, NP can potentially contain as high as 3560 ppm when NP directly contacts water. Since water molecules can hydrolytically degrade Estane, which ultimately degrades the chemical and mechanical properties of the polymer, the phase diagram of NP and water mixtures can be an important tool in estimating potential water concentration in NP.

Part Two: NP Thermal Stability in a Confined System

The stability of various classes of polynitro compounds has been investigated previously. However, relatively few studies have focused on understanding the decomposition pathways of BDNPA/F at temperatures below 70°C [12, 18, 19, 22-26]. Also, although numerous studies have focused on the aging behavior of the PBX9501 [12, 13, 16, 27-32], few have focused on the NP alone. From 2012 to 2014, we conducted thermal studies of NP aging over two years in headspaces containing air, nitrogen, or water to study how that headspace composition impacts the reaction pathway of the NP degradation. Those studies experimentally confirmed the mechanisms of NP degradation proposed by several research groups [33-35, 39]. It is known that the very first step in NP degradation is HONO formation, which then decomposes into NO_x, water, or HNO_x depending on the temperature and headspace condition. These reactive molecules can then serve as catalysts to accelerate the NP degradation. Therefore, the thermolysis of NP is often treated as a chaos degradation. The detailed degradation mechanisms and potential reactive intermediates at moderated temperatures can be found in references [1, 18, 19, 23, 25, 33-34].

Temperature and headspace composition are two major factors that impact NP aging behavior. Although temperature control is relatively easy to achieve, mimicking headspace conditions to simulate weapon applications is more difficult. In our earlier work, the aging containers had a large free volume (>30x the NP volume) [18, 19]. This was not representative of weapon conditions, where the systems are sealed with very little free volume. Also, the sampling procedure was such that a portion of the aged sample was withdrawn from the container for each of the various diagnostic characterizations after which the samples were resealed and returned for continued aging. This procedure resulted in a change in the concentrations of reactants and products in the headspace, stimulating further degradation of NP. This earlier work indicated the degradation of NP, even at temperatures below 38°C via changes in color and the FTIR spectra, but not in the NMR spectra [18, 19]. This was attributed to the change in the concentrations of reactants and products in the headspace and its large free volume. This observation was in contrast to the lack of observed degradation in the baseline NP, which has been stable for more than 50 years at Pantex ambient conditions when it was sealed in its original drum with a minimal headspace.
Therefore, to better mimic weapon application conditions, we conducted a new thermal aging study. Although the environmental conditions selected were the same as in the previous study, the free volumes of the aging devices were greatly reduced (free volume/NP volume <0.2) and the headspace composition was not allowed to freely exchange with the surrounding atmosphere during aging and sample removal processes. Since the detailed description about this aging study was given in several of recent manuscripts [35-37], only brief experimental/characterization descriptions and full results/discussion are given in this section of this report.

2.1. Aging Sample Preparation and Sample Characterization

In this study, NP used was obtained from a newly opened drum and past qualification tests conducted at Pantex. Its properties were characterized before aging in order to provide a baseline. For aging, this baseline NP was loaded into two different devices: IR cells for pseudo-in-situ near infrared (NIR) measurements and glass vials for TGA/KF/MIR/LCMS characterization, as shown in Figure 3. To perform these analyses, the baseline NP was also loaded into 20 IR cells and 240 vials. Over the aging period, the full suite of analyses was performed at 1, 2, 3, 4, 5, 6, 7, 8, 9, 10, 12, 15, 18, 21, 24, 28, 33, and 36 months during the study. A Thermo Nicolet™ iS50 FTIR spectrometer was used to conduct near

infrared (NIR) measurements in transmission mode between 4000 and 10000 cm^{-1} and MIR measurements in an attenuated total reflectance (ATR) mode with a diamond crystal between 4000 and 450 cm^{-1}. Prior to the measurement, the FTIR instrument was under N_2 purge for at least two hours to ensure baseline stability of the instrument. The OPUS/FTIR spectroscopy software package was used to analyze the NIR results and OMNIC™ Software was used to process the MIR results. For each sample, three to six spectra were collected, and the average result is reported. The KF titration was used to determine the water concentrations in the aged samples using a Mettler Toledo compact coulometric titrator.

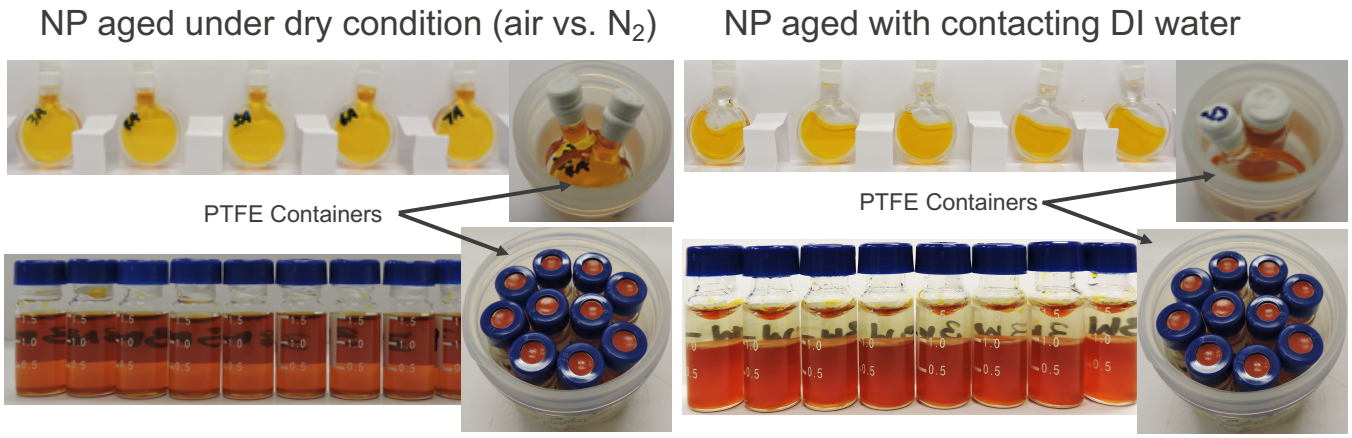

Figure 3. Photos of the NP samples prior to the artificial aging experiments.

2.2 Results Obtained from the Samples Aged under Air and Nitrogen

2.3.1 NIR Spectroscopy

Since NIR spectroscopy is widely used to detect trace amounts of water in the pharmaceutical and food industries, we applied this technique to our aged samples. Fig. 4 presents the NIR spectra of a set of samples aged inside the IR cells at 45°C for various times. For increased clarity, the water peaks at 5270 cm^{-1} are enlarged in an inset. Unlike the other peaks that are not sensitive to aging conditions, this water peak monotonically decreases as the time increases from 0 to 56 days. Similar changes are observed for the samples aged at other temperatures, but at different rates. These results suggest that water molecules leave the NP phase. Water molecules can accumulate in the headspace and/or escape out of the cells. Actually, when the cell is opened to air (<25RH%), the observed water peaks disappear within one day. The seal in the IR cells was imperfect, which allowed volatiles and water to escape at a very low rate. This allowed us to observe very subtle changes (< a few hundred ppms) over an extended period of time up to about 60 days and observe the property changes occurring at the very early onset of NP degradation. Using a set of NP/water standard solutions with pre-determined water concentrations, we constructed a calibration curve relating the areas of the water peaks in the NIR spectra to the water concentrations. The detailed description of construction of this calibration curve has been described in our earlier manuscripts elsewhere [8, 37]. This calibration curve, as shown in an inset in Fig. 5, was then used to calculate the water concentrations of the aged samples based on the water peaks in their NIR spectra. Fig. 5 presents the correlations between the calculated water concentration and time for six different temperatures. Over the course of the aging process, the water concentrations show three stages over time: 1) monotonic decrease; 2) slight fluctuation around a “mean” value without noticeable NP degradation (nondetectable using MIR); and 3) for the samples aged >55°C, a large fluctuation with noticeable NP degradation (detectable using MIR). As expected, the aging temperature impacts the slope and duration of each stage.

However, there seems to be a common phenomenon observed in these correlations, namely how the NP starts to degrade after its water concentration reaches the lowest point (a plateau) for a sustained period of time (after the second stage). It is known that NP contains a trace amount of water after its production [20]. The baseline NP used in this study contains ~760 ppm of water prior to the aging experiment. We suspect that as water diffuses out of the NP phases and reaches the lowest points at specific temperatures, as indicated by the flat lines in Fig. 6. Some NP molecules start to degrade through NP $\rightarrow$ NP' + HONO at moderate temperatures [33, 34]. As HONO decomposes into NO_x and water, this newly generated water compensates for the water lost through diffusion. When the diffusivity and production rate of water are comparable, the water concentration remains more or less constant, which may be responsible for the stability of the samples in the second stage. However, as the temperature increases, the rates of HONO formation and decomposition increase, as do the escape, evaporation, and auto-catalytic rates, which result in irreversible NP degradation. Actually, for the 70°C sample, due to the large rates, the water concentration almost approaches zero after 24 months of heating. The measurement of water concentration becomes unreliable because it approaches the instrument detection limit.

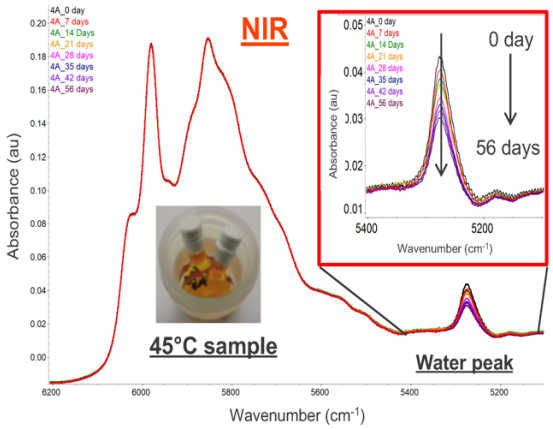

Figure 4. NIR spectra of a set of NP samples aged at 45°C from 0 to 56 days. Results between 4000 and 6500 cm-1 were shown. The water peaks were enlarged in an inset for better illustration.

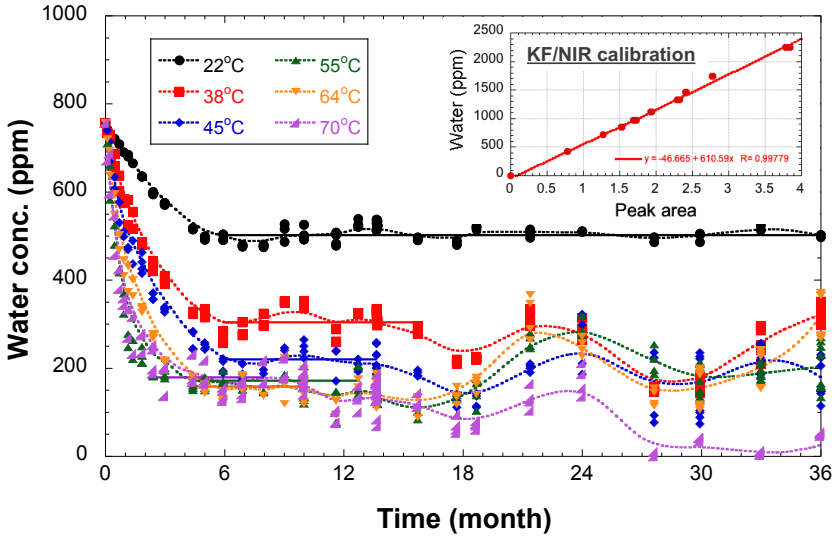

Figure 5. Correlation between water concentrations and time for the NP samples aged at various temperatures. Flat lines are used to indicate the "mean" values of the water concentrations in the aged samples during the second stage. The flat lines were drawn based on the mean values of water concentration between the flat regions. Inset is the KF/NIR calibration curve.

Our previous study found that when NP is sealed in its original drum with a minimal headspace, even after >50 years storage, chemical properties are preserved well and typically contains 600–800 ppm amount of water. Conversely, when the NP container is constantly exposed to a dry environment, such as that of Los Alamos (<50 RH%), the NP tends to lose this trace amount of water, and shows degradation at ambient temperature [20]. This observation might also explain why the NP degraded at 38°C and below within 24 months in our previous study, where the free volume was large and the headspace composition was periodically reset during the sampling [18, 19]. In this study, the composition does not freely exchange with its surroundings and, except for the water peaks, the NIR spectra remain almost the same for 36 months at temperatures below 55°C. This restriction seems to ensure the minimal requirement of the water concentration in NP for their stability. Although we are emphasizing the role of water here, we understand there are equilibrium requirements for the reactions of NP $\leftrightarrow$ NP' + HONO and HONO $\leftrightarrow$ NO_x + H_2O. Therefore, the concentration of NO_x in the headspace is critical as well. Since the water concentration is one of the measurable quantities in this experimental design, if we know the water concentration, we will know the NO_x concentration based on stoichiometry. At the very earliest stage of NP degradation, it is reasonable to assume there are no further reactions involved. Also, water can readily react with NO_x to form HNO_x, which is less volatile than NO_x. With these considerations, we believe that water concentration plays an important role in regulating the initiation of NP degradation at lower temperatures.

It is worth noting that in the previous studies, it was determined that the headspace atmosphere significantly altered the reaction pathway of the NP thermal degradation [18, 19]. When we designed the current study, we prepared air and N_2 samples, and expected to see different aging behaviors. However, the NIR results reveal an insignificant difference between these two sets of samples as shown together in Fig 5. We reason that this lack of a significant difference is due to the low free volume (<0.03 ml) in the cell, as shown in Fig. 2. The oxidants, such as NO_x, generated from the NP degradation dominate the aging behavior of NP, and diminish the initial different compositions in the headspace. A similar observation was reported by Wewerka et al. in 1976 when they aged PBX 9501 in systems with low free volume under different environments. They believed that the attacking species must have been produced in situ [21].

2.3.2 KF Measurement

As shown in Fig. 6, the water concentrations of the air and N_2 samples aged inside the glass vials were directly measured using KF titration. Initially, all samples behave similarly. Their water concentration decreases to the lowest value and then starts to fluctuate for extensive period of time. After 12 months, the water concentrations in the 64°C samples increase with time. Actually, after 33 and 36 months, the water concentrations in the 55°C samples also increase. Both results suggest that samples aged at temperatures above 55°C demonstrate different aging behaviors than those aged at temperatures below 55°C. We speculate that the auto-catalytic reaction starts to dominate the NP degradation, which causes cascading reactions and results in the irreversible changes in the NP properties. Interestingly, the turning points for the air and N_2 samples occur at different times when the samples are aged inside the glass vials. We suspect that this difference may be attributed to three sources: 1) the free volume in the glass vials (~20%) are larger than that in the IR cells (~10%) compared to the NP sample volume; 2) the vials were overall sealed better than the cells; and 3) the vails were kept in their own PTFE containers (air or nitrogen) over the entire aging experiment. Therefore, even though there was the possibility of leaks due to the deterioration of the caps, the composition in the headspace in the vial samples were better preserved. As

a result, the initial composition in the headspace shows some impact on the aging behavior of NP, but not as significant as we found in the previous work [18, 19].

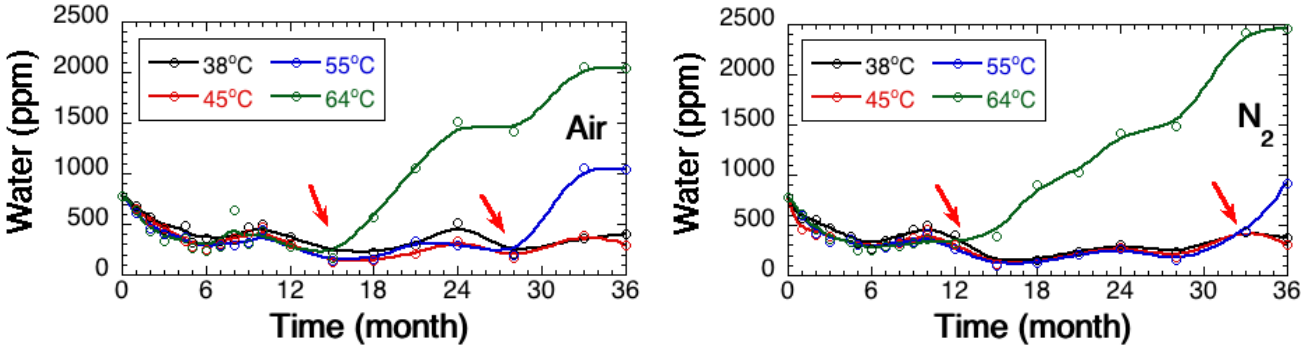

Figure 6. Effect of temperature and time on the water concentration in the air and N_2 samples. as the acidity of the aged sample increases, the measurement of KF becomes less accurate though the largely increased water concentrations in the 55 and 64°C samples are still evidenced.

Overall, these KF results are consistent with the results obtained from the samples aged inside the IR cells, as shown in Fig. 6. It is especially true at the early stages of the aging experiment. As the aging progresses, the difference between these two sets of results becomes more obvious, which is most likely due to imperfect seal for the cells. The prolonged aging results in more severe loss of water and NO_x escaping from the cells. Their depletion not only triggers HONO decomposition moving forward and but also reduces the concentration of oxidants in the headspace. Conversely, most volatiles accumulate in the headspace of the vials. At low temperatures, these accumulated products may slow down HONO formation, but at elevated temperatures, their accumulation enhances their chance to attack the degraded NP though the auto-catalytic effect, which may explain why the transition points come earlier in the samples aged inside the vials than for those aged inside the cells. Therefore, headspace composition plays a critical but complex role in changing the pathways and rates of the NP degradation.

2.3 Results Obtained from the Samples Aged in Direct Contact with Water

For this study, the NP samples in direct contact with water during aging are referred to as "wet" samples. During PBX 9501 production and its later characterization, the material is often directly in contact with water. Also numerous artificial aging experiments of PBX 9501 were conducted under high humidity (up to 74%RH) at 70°C by many researchers [27-29, 38-40]. The NP was aged in direct contact with water molecules. While extensive characterization was conducted on aged PBX 9501 as a whole, how NP degrades under this kind of condition has been rarely reported. In our previous study [19], while the properties of aged samples were characterized using TGA/FTIR/NMR/LC-MS, their water concentrations were not measured. Figure 7 presents the water concentration of these NP samples over time. Initially, the water concentration increases from 780 ppm to >2500 ppm, depending on the temperature. After ~6 months, the water concentration reaches a plateau (saturation) at a specific temperature. The water concentration then remains constant for more than 36 months for all samples except for the sample aged at 64°C, in which the water concentration increases with time. Even under this super-saturated water condition, the auto-catalytic reaction seems to dominate the NP degradation and results in the irreversible degradation at elevated temperatures.

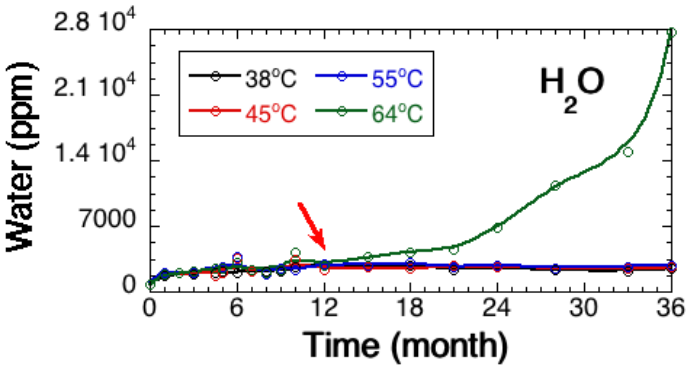

Figure 7. Effect of temperature and time on the water concentration in the wet NP samples.

2.4 MIR Spectra of Long-Term Aged NP Samples

Figure 8 presents the MIR spectra of baseline NP and the NP samples aged at 6 and 28 months and at 55°C and 64°C in air and under water, respectively. For more clarity, the MIR spectra were divided into high wavenumber (HWN) and low wavenumber (LWN) regions. As expected, when NP is aged in contact with water for 6 and 28 months at 55°C, the NP samples contain some degradation products and more water than the baseline NP. This is shown in the water peak between 3800–3100 cm^{-1} and the hydrogen stretch in the HNO_3 environment peak at 3590 cm^{-1} [41, 42]. These newly formed peaks confirm the presence of HNO_3. The higher intensity in the 28-month sample than that in the 6-month sample suggests more HNO_3 molecules in the longer aged sample. Other than that, the overall spectral changes in the rest of this region are not significant. For the samples aged at 45°C and below, up to 36 months, there are no noticeable changes in entire FTIR region (not shown here).

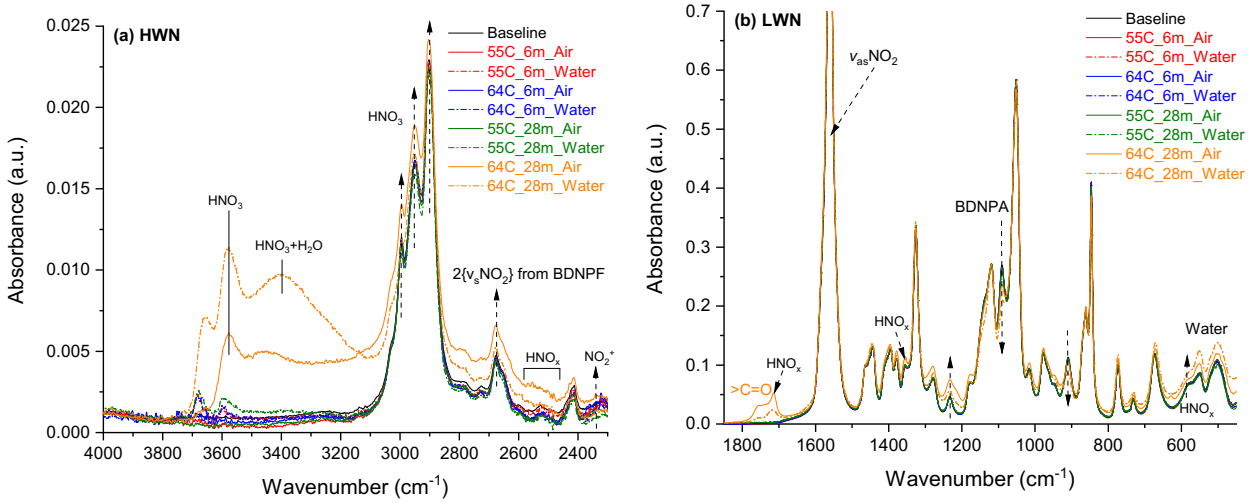

Figure. 8. MIR of baseline NP and various aged NP samples. (a) HWN region and (b) LWN region.

For the 6-month samples aged at 64°C in water, the peaks similar to those found in the 55°C samples are observed between 3800–3100 cm^{-1}. However, after 28 months of aging, these peaks significantly increase in intensity. The NP samples aged in air also show large differences between 6 and 28 months. As expected, the dry and wet environments result in different forms and concentrations of $HNO_3 \bullet nH_2O$ and NO_x in the aged samples. Their characteristic peaks can be seen across the entire MIR region. Additionally, the -CH_n peaks (between 3100–2800 cm^{-1}) and >CH-OH/CH-NH (between 3500–3100 cm^{-1}) broad bands change in their intensities as the aging time increases from 6 to 28 months. The

large intensity of the >CH-OH/CH-NH in the NP aged under water confirms the formation of C-OH and C-NH [19]. In the LWN region, a ketone >C=O peak emerges between 1800–1700 cm^{-1} in both the wet and dry NP samples along with the characteristic band of HNO_3 vapor at 1710 cm^{-1} [41]. The intensity of this band in the dry sample is larger than that in the wet sample due to the dilution by water in the wet sample. The intensities of other peaks also evolve differently in these two samples, which suggest that NP degrades differently when it is exposed to air or water. Overall, the MIR spectral results are consistent with the KF results, confirming the formation of new chemical species in the NP samples aged at 55°C and above, but not in the samples aged below 55°C after 36 months of aging. Also, it should be noted that the BDNPA peak in the FTIR decreases more than the BDNPF peak, which confirms previous findings that BDNPA is more prone to degrading than BDNPF [18, 19].

2.5.Conclusion

In this study, a systematic aging experiment was carried out, investigating the stability of NP when the free volumes in the aging containers were small. This study is are more relevant to weapon applications than previous studies. These results suggest at <55°C, NP is stable when it contains a trace amount of water, which seems to prohibit the formation of HONO. Additionally, when NP is in direct contact with water and the aging temperature is increased, its water solubility increases, although its stability is not necessarily compromised at low temperatures. However, at >55°C, NP degradation starts within a few months regardless of the composition of the aging atmosphere. We suspect that the generated NO_x, water, and HNO_x can serve as catalysts to accelerate NP degradation so that NP degradation becomes an auto-catalyzed reaction and results in an irreversible degradation.

Since the amount of water (and volatiles) involved in the initial degradation of NP is on the order of a few hundred ppms it is critical to rigorously control headspace volume in addition to ageing temperature to study the aging behavior of NP and NP containing materials, such as PBX 9501. Particularly so in a relatively dry environment, such as that at LANL. Over the past two decades, numerous artificial aging experiments of PBX 9501 and polymeric materials containing NP have been conducted in the DOE complex at temperatures up to 80°C without and with humidity (up to 75 RH%), often with a large headspace volume in aging containers, and sometimes with an extra NP source. Although invaluable knowledge has been accumulated about the aging behaviors of these materials from these studies, the uncovered aging behaviors are not necessarily relevant to applications in the LANL weapon systems. We hope that the results obtained from this new study shed some light on the conditions at which NP degradation starts and provides experimental evidence which may help to design future artificial aging studies related to the materials containing NP under the conditions more relevant to the weapon conditions.

Part Three: Characterization of BDNPA/F using newly installed LC-QTOF

Standard HPLC with Diode Array Detection is unable to determine the products from the degradation of BDNPA, BDNPF, and NP. In FY2018, we purchased a high resolution HPLC/MS/MS system - SCIEX X500r liquid chromatography tandem quadrupole time of flight mass spectrometer (LC-QTOF) instrument. In FY2019, we focused on the methodology development for BDNPA/F and degradation product characterization. Preliminary results are reported in this section.

3.1 Method Development

With method development still underway, multiple configurations of instrument parameters, mobile phase properties, and stationary phases. Conditions using methanol, acetonitrile, water with 0.1% ammonium formate, water with 0.1% ammonium formate, water with 0.1% acetic acid, and water with 0.1% acetic acid, have all been attempted with varying degrees of success. The greatest success has been using: 95% optima grade acetonitrile (ACN) with 5% optima grade methanol (MeOH) with 0.1% ammonium acetate as the organic mobile phase (phase B) and optima grade deionized water (DI) with 0.1% ammonium acetate as the aqueous mobile phase (phase A). Flow volume is set to 0.3 mL/min with a gradient from 10% phase B to 99.9% phase B back to 10% phase B over 10 minutes, with a C8 reverse phase column held at 40°C. Rinsing the system with acetone between each sample analysis also plays an important role in reducing the possibility of column bleed. The separated analytes are introduced to the mass spectrometer via positive and negative electrospray ionization (ESI), and analyzed utilizing information dependent acquisition (IDA) set to acquire MS/MS data when response for any mass channel is greater than 1000cps, the samples are evaluated from 20m/z to 650m/z. In early work it was established for NP, analysis from 500 to 5000m/z yields few results, for this reason the analysis was limited to 20 to 650 m/z.

3.2 Sample Preparation

As of now, 288 samples have been collected and retained at LANL, the samples are 16 each (three NP conditions: air, nitrogen, water, this also includes the water used to saturate the NP; at four temperatures 38°C, 45°C, 55°C, and 64°C), these samples were collected at 18 time periods. The samples are aged under the conditions above, after the aging is completed, the samples are held refrigeration at <6°C. Before injection, the samples are diluted 1:1000 (vol:vol) in 1:1 (vol:vol) ACN:H_2O, for the water saturated samples the analyst is careful not to draw sample from areas of the sample where droplets of water have formed in the heterogeneous solution. Experimental parameters are being determined using the 12, 24, and 36 month water exposed NP samples at each temperature.

3.3 Results and Discussion

In every analysis, hundreds of masses detected in an aged NP sample, the majority of these detections do not have refined chromatography parameters and are considered background. By individually evaluating each chromatogram for each detected mass channel (1000-4000 per sample), peaks out of the background can be identified and real data sorted from background.

Mass channels which have Gaussian peaks for elution volume include: -45.671, -61.7197, -119.0452, -141.1964, -348.8549, -373.1157, -387.2535, +140.9614, +174.9614, +228.1955, +259.0533, +268.9980, +304.0739, +335.0426, +349.0612, and +433.0032 m/z (sign denotes ESI mode). Molecules

that have Gaussian peaks for elution volume and justifiable mass spectra include: BDNPF, BDNPFA, and ONO^- found at +335.0426m/z, 0.79min; +349.0612m/z, 0.77min; and -45.671m/z, 8.9min respectively.

In Fig. 9, the hydrocarbon based Kendrick Mass Defect (KMD) plot is shown for all signals, which had clear chromatographic peaks. The KMD plot was determined based on one of hydrocarbons as a single methyl, which is difference between BDNPA and BDNPF. As shown in Fig. 9, two points show horizontality and separation of 14 Da in nominal Kendrick mass, demonstrating the two molecules the points represent differ only by this methyl group. The exact masses, shown in Fig. 9(B) were determined to be the $[M+Na]^+$ adducts of BDNPA and BDNPF, as shown in Table 2.

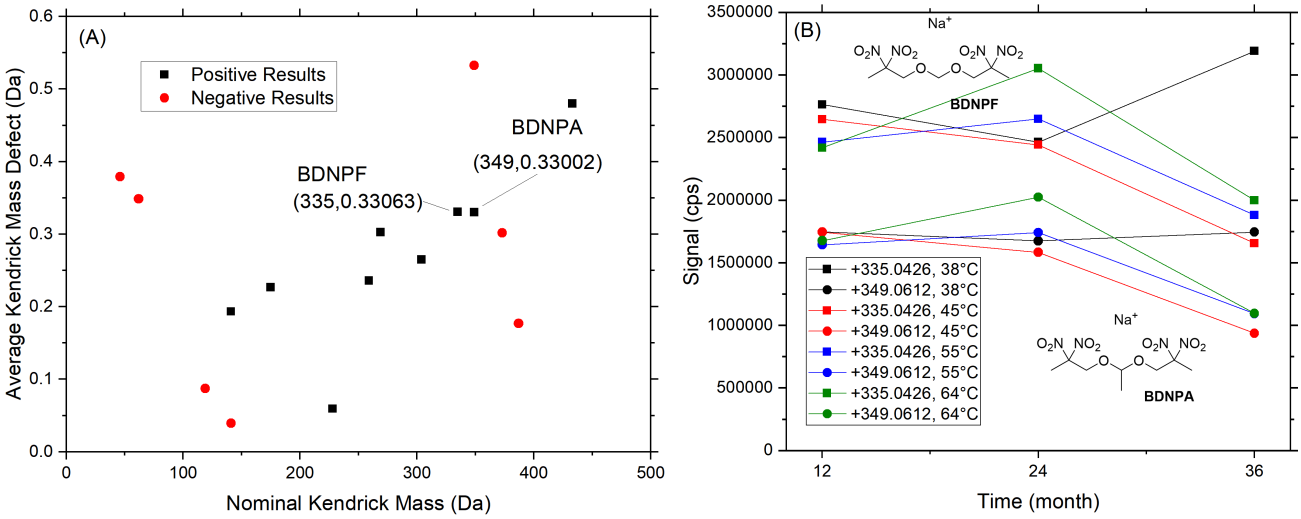

Figure 9. (A) Hydrocarbon derived KMD plot for all chromatographic peaks detected in NP samples exposed to water for 12, 24 and 36 months, the marked peaks show the same average KMD (to three decimal places) and represent the sodium adducts of BDNPA/F. (B) Changes in signal in each sample for BDNPA-Na^+ and BDNPF-Na^+.

Table 2: Theoretical exact masses compared to measured mass channels.

Molecule	**Formula**	**Exact Mass**	**[M-Na]+**	**Measured m/z**
BDNPA	$C_7H_{12}N_4O_{10}$	312.0553	335.0446	335.0426
BDNPF	$C_8H_{14}N_4O_{10}$	326.0710	349.0602	349.0612
Na+	Na+	22.9892		

In previous and this work we have suspected the formation of nitrous acid (HONO) in aged NP. We have detected this molecule in the aged NP samples here as the nitrite ion $[NO_2]^-$, as shown in Figure 10. The discrepancy between measured mass and exact mass is consistent with that of the acetate ion. The exact mass of the formate ion has the same discrepancy as shown in Table 3. Interestingly, as shown in Fig. 10, the nitrite signal is lower in the samples aged above 55°C, however the signal increases dramatically at 24 months for the 64°C sample, whereas the concentration of $[NO_2]^-$ in the sample aged at 55°C remains quite low until 24 months, and then increases at 36 months. The concentration of $[NO_2]^-$ in the 38°C sample remains relatively constant through the entirety of the experiment, whereas its concentration in the 45°C sample initially remains similar to that in the 38°C sample and then drops to nearly zero at 36 months. Many reasons can result in the concentration of $[NO_2]^-$ changing with temperature and aging time. Among those reasons, it is most likely related to HONO generation rate and

its solubility in NP and water associated with different temperatures. It is suspected that the solubility of $[NO_2]^-$ in water increases with increasing temperature and $[NO_2]^-$ concentration. When the NP samples were aged in contact with water, due to its possible increased solubility in water with temperatures, water is able to effectively extract the $[NO_2]^-$ into the aqueous phase, the concentration of $[NO_2]^-$ in the NP phase decreases at 64 and 55°C compared to that in the NP aged at 38 and 45°C initially. However, since the degradation rate of NP increases with increasing temperature, as more and more HONO is generated and accumulated in both aqueous and NP phases, the concentration of $[NO_2]^-$ increases with time at the elevated temperatures, such as 64°C. We predict that the concentration of $[NO_2]^-$ in NP will increase with time as NP is continuously aged at 55°C. On the other hand, the decreased $[NO_2]^-$ in the NP aged at 45°C might be due to its extraction by the water phase as the $[NO_2]^-$ concentration increases in the aqueous phase. We predict that the prolonged aging will make the $[NO_2]^-$ concentration increase in all temperatures, just at different rates. Clearly, to verify our suspicions, we are analyzing the $[NO_2]^-$ concentration in the corresponding aqueous samples.

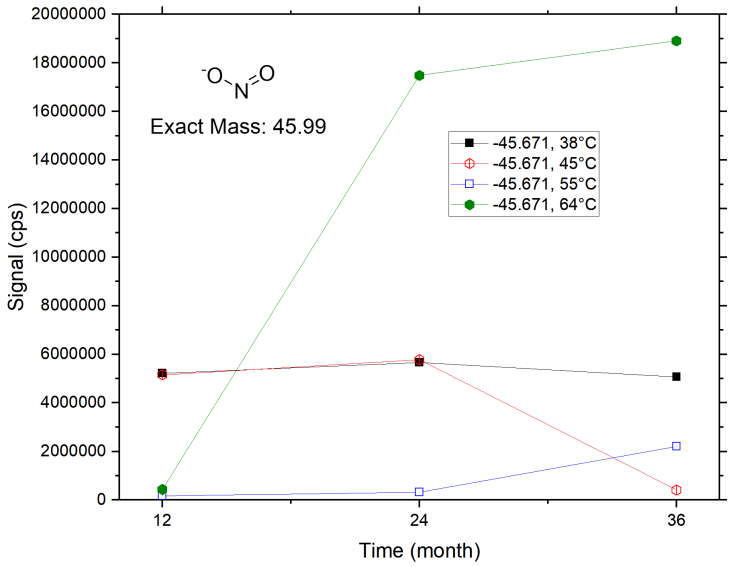

Figure 10: The signal change in nitrite ions are shown for the NP samples aged at 12, 24, and 36 months in contact with water at four temperatures.

Table 3: Theoretical exact masses compared to measured mass channels, % Difference compares differences between exact and measured mass, showing the differences between formate and nitrite ions.

Molecule	**Formula**	**Exact Mass**	**Measured m/z**	**Difference**
ONO-	ONO-	45.9929	45.6710	0.3219
Formate-	CHOO-	44.9982	44.6750	0.3232
			% Difference	**0.2015%**

We will continue to develop and refine the methodology, and then analyze full set of 288 samples collected over the past three years. Together with other characterization techniques as described in Part Two, we should have more comprehensive understanding about how NP thermally degrades under various environments.

ACKNOWLEDGMENTS

This work was supported by the US Department of Energy through the Los Alamos National Laboratory Aging and Lifetimes Program. Los Alamos National Laboratory is operated by Triad National Security, LLC, for the National Nuclear Security Administration of the U.S. Department of Energy (Contract No.89233218NCA000001).

REFERENCES

[1] R. B. Rauch, Behrens, R., Vapor Pressures, Mass Spectra and Thermal Decomposition Processes of Bis(2,2-dinitropropyl) Acetal (BDNPA) and Bis(2,2-dinitropropyl) Formal (BDNPF), Propellants, Explosives, Pyrotechnics 32(2) (2007) 97-116.

[2] M. R. Salazar, Lightfoot, J. M., Russell, B. G., Rodin, W. A., McCarty, M., Wrobleski, D. A., Orler, E. B., Spieker, D. A., Assink, R. A., and Pack, R. T., Degradation of a Poly(ester urethane) Elastomer III. Estane 5703 Hydrolysis: Experiments and Modeling, Journal of Polymer Science: Part A: Polymer Chemistry 41 (2003) 1136–1151.

[3] S. K. Shee, Reddy, S. T., Athar, J., Sikder, A. K., Talawar, M. B., Banerjee, S., Khan, M. A. S. , Probing the compatibility of energetic binder poly-glycidyl nitrate with energetic plasticizers: thermal, rheological and DFT studies RSC Adv. (2015) 101297-101308.

[4] S. M. Shen, Leu, A. L., Yeh, H. C., Thermal Characteristics of Polyurethane PEG and BDNPA F-Blends, Thermochim. Acta 176 (1991) 75.

[5] N. Wingborg, Eldsäter, C., 2,2-Dinitro-1,3-Bis-Nitrooxy-Propane (NPN): A New Energetic Plasticizer. Propellants, Explosives, Pyrotechnics, 27 (2002) 314-319. doi:10.1002/prep.200290000

[6] E. B. Orler, Wrobleski, D. A., Cooke, D. W., Bennett, B. L., Smith, M. E., Jahan, M. S., Thermal Aging of Nitroplasticized Estane 5703 No. LA-UR-02-1315, Los Alamos National Laboratory (2002).

[7] T. Rivera, Study to Determine the Phase Diagram of the BDNPA/F System, LA-05313, Los Alamos Scientific Laboratory of the University of California, 1973, p. 2.

[8] A. Edgar, Yang, J., Chavez, M., Yang, M., Yang, D., Physical Characterization of Bis(2,2-dinitropropyl) Acetal and Formal, J. of Energic Material, DOI: 10.1080/07370652.2020.1737987, 2020.

[9] S.-M. Shen, Leu, A.-L., Yeh H.-C., Thermal Characteristics of Polyurethane PEG and BDNPA/F Blends, Thermochimica Acta 176 (1991) 13.

[10] D. J. Idar, Thompson, D. G., Gray III, G. T., Blumenthal, W. R., Cady, C. M., Peterson, P. D., Roemer, E. L., Wright, W. J., Jacquez, B. J., Influence of Polymer Molecular Weight, Temperature, and Strain Rate on the Mechanical Properties of PBX 9501 AIP Conference Proceedings 620(1) (2002) 821.

[11] D. W. Brown, Lowry, B. W., Smith, L. E., Kinetics of hydrolytic aging of polyester urethane elastomers. Macromolecules 13(2) (1980) 248-252.

[12] M. R. Salazar, Kress, J. D., Lightfoot J. M., Russell, B. G., Rodin, W. A., Woods, L., Low-temperature Oxidative Degradation of PBX 9501 and its Components Determined Via Molecular Weight Analysis of the Poly(ester urethane) Binder., Polymer Degradation and Stability 94 (2009) 2231-2240.

[13] M. R. Salazar, Kress, J. D., Lightfoot, J. M., Russell B. G., Rodin W. A., Woods, L, Experimental Study of the Oxidative Degradation of PBX 9501 and its Components, Propellants, Explosives, Pyrotechnics 33(3) (2008) 182-202.

[14] D. Yang, A simple kinetic model for early onset degradation of nitroplasticizer, LA-UR-18-23458, Los Alamos National Laboratory 2018.

[15] M. R. Salazar, Thompson, S. L., Laintz, K. E., Pack, R. T., Degradation of a Poly(ester urethane) Elastomer I. Absorption and Diffusion of Water in Estane 5703 and Related Polymers, Journal of Polymer Science: Part B: Polymer Physics 40 (2002) 181-191.

[16] M. R. Salazar, Pack R. T., Degradation of a Poly(ester urethane) Elastomer II. Kinetic Modeling of the Hydrolysis of a Poly(butylene adipate), Journal of Polymer Science: Part B: Polymer Physics 40 (2002) 192-200.

[17] M. R. Salazar, Thompson, S. L., Laintz, K. E., Meyer, T. O., Pack R. T., Degradation of a Poly(ester urethane) Elastomer IV. Sorption and Diffusion of Water in PBX 9501 and its Components, Journal of Applied Polymer Science 105 (2007) 1063-1076.

[18] D. Yang, Pacheco, R., Edwards, S., Henderson, K., Wu, R., Labouriau, A., Stark, P., Thermal Stability of a Eutectic Mixture of Bis(2,2-dinitropropyl) Acetal and Formal: Part A. Degradation Mechanisms in Air and Under Nitrogen Atmosphere, Polymer Degradation and Stability 129 (2016) 380-398.

[19] D. Yang, Pacheco, R., Edwards, S., Henderson, K., Wu, R., Labouriau, A., Sykora, M., Stark, P., Larson, S., Thermal Stability of a Eutectic Mixture of Bis(2,2-dinitropropyl) Acetal and Formal: Part B. Degradation Mechanisms Under Water and High Humidity Environments, Polymer Degradation and Stability 130 (2016) 338-347.

[20] D. Yang, Torres, J., Cluff, K., Adams, J., Edgar, A., Stability of Naturally Aged Nitroplasticizer, LA-UR-18-23141, Los Alamos National Laboratory 2018, p. 17.

[21] E. M. Wewerka, Loughran, E. D., Williams, J. M., The Effects of Long-Term Storage at Elevated Temperatures on Small Cylinders of PBX 9501, Los Alamos Scientific Laboratory, Los Alamos Scientific Laboratory, 1976, p. 13.

[22] C. F. Melius, Piqueras, M. C., Initial Reaction Steps in the Condensed-Phase Decomposition of Propellants, Proceedings of the Combustion Institute 29 (2002) 2863-2871.

[23] K. F. Mueller, Renner, R. H., Gilligan, W. H., Adolph, H. G., Kamlet, M. J., Thermal Stability/Structure Relations of Some Polynitroaliphatic Explosives, Combustion and Flame 50 (1983) 9.

[24] Y. Oyumi, Brill, T.B., Thermal Decomposition of Energetic Materials 11. Condensed Phase Structural Characteristics and High Rate Thermolysis of Di- and Trinitroaliphatic Carboxylic Acids and Carbonates, Combustion and Flame 65 (1986) 9.

[25] R. Shaw, Heats of Formation and Kinetics of Decomposition of Nitroalkanes, International Journal of Chemical Kinetics 216-269 (1973) 9.

[26] H. G. Adolph, Evidence for Rate-Determining C-C Bond Heterolysis in the Condensed Phase Thermal Decomposition of Polynitroethyl Compounds, Combustion and Flame 70 (1987) 5.

[27] D. Wrobleski, Langlois, D., Orler, E., Dattelbaum, D., Small, J., Application of 15N labeling for oxidative degradation study of a plasticized poly(ester urethane), Polymer Preprints 45(1) (2004) 2.

[28] D. A. Wrobleski, Langlois, D. A., Orler, E. B., Schoonover, J. R., Small, J. H., Thermal degradation studies of nitroplasticized estane [Registered] 5703 utilizing isotopic enrichment, LA-UR-02-3428, Los Alamos National Laboratory, Los Alamos, New Mexico, 2002.

[29] J. D. Kress, Wrobleski, D.A., Langlois, D.A., Orler, E. B., Lightfoot, J. M., Rodin, W. A., Huddleson, C. O., Woods, L., Russell, B. G., Salazar, M. R., Paular, D. K., Aging of PBX 9501 Binder and Free-Radical Oxidation, 27th Compatibility, Aging and Stockpile Stewardship Conference, LA-UR-06-6630, Los Alamos, New Mexico, 2006.

[30] D. G. Thompson, Accelerated vs. Stockpile Aging of PBX 9501: A Summary of Three Enhanced Surveillance Studies, in: DOE (Ed.) 27th Aging Compatibility and Stockpile Stewardship Conference, LA-UR-06-6723, Los Alamos, New Mexico, 2006, p. 16.

[31] M. R. Salazar, J. D. Kress, J. M. Lightfoot, B. G. Russell, W. A. Rodin, L. Woods, Experimental Study of the Oxidative Degradation of PBX 9501 and its Components, Propellants, Explosives, Pyrotechnics 33 (2008) 20.

[32] J. D. Kress, Wrobleski, D. A., Langlois, D. A., Orler, E. B., Labouriau, A., Uribe, A., Houlton, R., Kendrick, B., Aging of the Binder in Plastic-Bonded Explosive PBX 9501 and Free Radical Oxidation, in: M. C. Celina, J. S. Wiggins, N. C. Billingham (Eds.) Polymer Degradation and Performance, ACS, 1155 16th St. NW, Washington, DC 20036 USA, 2009, pp. 181-196.

[33] C. F. Melius, Piqueras, M. C., Initial Reaction Steps in the Condensed-Phase Decomposition of Propellants, UCRL-JC-146559, Lawrence Livermore National Laboratory, 2001, p. 31.

[34] D. K. Pauler, Henson, N. J., Kress, J. D., A mechanism for the decomposition of dinitropropyl compounds, Physical Chemistry Chemical Physics 9(37) (2007) 5121-5126.

[35] D. Yang, Adams, J., Edgar, A., Torres, J., Yang, J., Study of Nitroplasticizer Stability, J. of Weapon Engineering, submitted Dec. 2019.

[36] K. D. Morris, Aged Nitroplasticizer Study, PXRPT 19-18, Consolidated Nuclear Security, llc. Pantex Plant, Amarillo, TX, 2019, p. 55.

[37] D. Yang, Zhang, D.Z. Role of water in degradation of nitroplasticizer, Polymer Degradation and Stability, 170 (2019) 109020.

[38] D. G. Thompson, Deluca, R., Accelerated Aging of PBX 9501 from Universal Hemispheres, Los Alamos National Laboratory Report: LA-CP-14-00015, Los Alamos, New Mexico, 2014, p. 20.

[39] D. G. Thompson, DeLuca, R., Quasi-Static Tension and Compression of Pressed PBX 9501 After Accelerated Aging, the 25th Aging, Compatibility and Stockpile Surveillance Conference, LA-UR-03-8466, Los Alamos National Laboratory, Lawrence Livermore National Laboratory, Livermore CA, 2003.

[40] D. A. Wrobleski, Langlois, D. A., Orler, E. B., Labouriau, A., Uribe, M., Houlton, R., Kress, J. D., Kendrick, B., Accelerated Aging and Characterization of a Plasticized Poly(ester urethane) Binder, in: M.C. Celina, J.S. Wiggins, N.C. Billingham (Eds.) The 233rd National Meeting, American Chemical Society, Polymer Degradation and Performance, American Chemical Society, Chicago, IL, 2008, p. 15.

[41] R. A. Marcus, Fresco, J. M., Infrared Absorption Spectra of Nitric Acid and Its Solution, The Journal of Chemical Physics 27(2) (1957) 5.

[42] O. Redlich, Nielsen, L. E., Raman Spectrum and Molecular Vibrations of Nitric and Deuteronitric Acids, JACS 65 (1943) 7.